de Haas–van Alphen Effect in n InSb

R. J. Sladek*†
Department of Physics, Purdue University, Lafayette, Indiana 47907
and
E. R. Gertner
Science Center, North American Rockwell Corporation, Thousand Oaks, California 91360
and
D. G. Seiler
Department of Physics, North Texas State University, Denton, Texas 76203
(Received 11 June 1970)

Measurements of de Haas–van Alphen torque oscillations have been made at 1.2 K on single-crystal n-type InSb samples containing between 6.6×10^{17} and 4.5×10^{18} electrons/cm^3. The amplitude of the oscillations is found to depend on the crystallographic orientation and magnitude of the magnetic field. The anisotropy is accounted for by the warping of the conduction band and the damping by collision and inhomogeneity broadening. From the anisotropy of the period of the highest-concentration sample, we obtain $L-M-N=(8.9\pm0.7)\hbar^2/2m_0$.

I. INTRODUCTION

The de Haas–van Alphen (dHvA) effect (oscillatory dependence of the magnetic susceptibility on the reciprocal of the magnetic field strength) has been used extensively to investigate the Fermi surfaces of metals. The related Shubnikov–de Haas (SdH) effect (oscillatory magnetoresistance) has provided more information about the band structures of degenerate semiconductors[1] including some on the anisotropy of the conduction band in InSb.[2,3] In this paper, we present detailed results of an experimental study of the dHvA torque oscillations in samples of n-type InSb.[4] The anisotropy we observe will be interpreted by means of a theoretical expression for the extremal cross-sectional area of the Fermi surface derived[1] employing Kane's three-band approximation.[5] A value for the warping parameter $(L-M-N)$ will be deduced. When inversion asymmetry effects are negligible, all the anistropy of the primary conduction and valence bands is proportional to $L-M-N$. The interactions between the various energy states which give rise to $L-M-N$ are discussed in Ref. 5. The dependence of the amplitude of the oscillations on field strength will be analyzed in terms of collision[6,7] and inhomogeneity[6] broadening of the Fermi energy.

II. EXPERIMENTAL

The samples were cut, lapped, and etched with their long dimension parallel to within $\pm\frac{1}{2}^\circ$ to the [110] direction from Te-doped n-type InSb purchased from Cominco American, Spokane, Washington. They are identified and characterized in the tables. The Hall effect and resistivity were measured at 4.2 K using conventional dc potentiometric techniques. The dHvA measurements were made with the samples suspended vertically in liquid helium at about 1.2 K. (Attempts to obtain dHvA data at 4.2 K were unsuccessful because of the bubbling of the liquid-helium bath.) The outputs of a null-deflection torsion apparatus[9,10] and a rotating-coil gaussmeter were plotted on a Moseley x-y recorder as the field of a 22-in. Varian magnet was swept automatically through a convenient range. The gaussmeter was calibrated with a standard magnet.

III. RESULTS

Hall-effect and Hall-mobility data are given in Tables I and II, respectively. Also included in Table I are values of various parameters deduced from the Hall data and formulas given in the text or in the literature. These parameters are used below in analyzing the anisotropy and field dependence of our dHvA torque oscillations.

Various results of our torque measurements are given in Figs. 1 and 2 and Tables III and IV. Figure 1 shows a reproduction of the x-y recorder tracing for a number of orientations of the magnetic induction $\vec{B}$ for the lowest concentration sample. Similar tracings were obtained for samples 2 and 3. For sample 3, the period depended on the orientation of $\vec{B}$ and will be discussed below. In all samples the oscillations were periodic in $1/B$ and the measured periods are listed in Table III. For comparison, the periods calculated from the Hall effect employing Eq. (6) are also listed there. The agreement is probably satisfactory since one does not know how to calculate the carrier concentration exactly from the Hall effect. To within the accuracy of our measurements, the torque oscillations were found to be damped exponentially like $e^{-\alpha/B}$. Although theory[11] predicts that an additional field-dependent factor multiplies the exponential [see Eq.

TABLE I. Characteristics of n-InSb samples[a] derived from R_H the Hall coefficient measured at 4.2 K and formulas for electron wave vector k, energy E, and g factor (see text and Ref. 5). S is the extremal cross-sectional area of a surface of constant energy when anisotropy and inversion asymmetry effects are neglected.

Slice designation[b]	$1/\lvert R_H e\rvert$ [b] (10^{18}/cm^3)	k_F (10^6 cm^{-1})	ζ (eV)	$dS/d\zeta$ (10^{26}/erg cm^2)	$-g$
$W326$-J	0.66	2.68	0.124	1.51	23
$W324$-H	1.11	3.19	0.161	1.71	19
$W226$-H	4.5	5.10	0.311	2.54	10

[a] The samples used for the dHvA torque measurements were from the same slices as the Hall samples.
[b] The slice designations are those of the supplier, Cominco American, Spokane, Wash.

(4)], we do not regard the discrepancy as important because the factor has a much weaker field dependence than would be detectable over the range of B which we employed. The maximum amplitude of the oscillations at a specific field strength and the damping constant α for each sample are listed in Table IV.

IV. DISCUSSION

A. Anisotropy and Period

In order to interpret the period and anisotropy of our dHvA oscillations, we shall reproduce below some pertinent results from Ref. 1. Specifically, the extremal cross-sectional area S_m of a surface of constant energy in the Γ_6 conduction band of InSb is given by

$$S_m = \pi C_0[1 - C_1 g_1(\Theta)/2\pi] . \quad (1)$$

C_0 and C_1 depend only on the energy and the band parameters as indicated in the Appendix. When, as in our experiment, the magnetic induction $\vec{B}$ is in the (110) plane, the function $g_1(\theta)$ is given by[1]

$$g_1(\theta) = \tfrac{1}{16}\pi[8 - (-1 + 3\cos^2\theta)^2] , \quad (2)$$

where θ is the angle between the direction of $\vec{B}$ and the [001] crystal direction.

From Eqs. (1) and (2), we have

$$\frac{\partial S_m}{\partial \theta} = -\tfrac{3}{8}\pi C_0 C_1 \sin\theta\cos\theta(-1 + 3\cos^2\theta) . \quad (3)$$

TABLE II. Parameters pertinent to the damping of the dHvA torque oscillations. μ_0 is calculated from $\lvert R_H\rvert/\rho_0$ using Hall and resistivity data at 4.2 K. The screening parameter q_0, the ratio of the lifetime of a carrier on the Fermi surface τ to the resistivity relaxation time τ_ρ, the collision damping parameter α_c (calc), and the inhomogeneity broadening temperature T_i are deduced as indicated in the text.

Sample n InSb	μ_0 (cm^2/V sec)	q_0 (10^6 cm)	$\frac{\tau}{\tau_\rho}$	α_c(calc) (kG)	T_i (K)
1	35 000	1.0	0.175	51	17
2	26 000	1.15	0.165	73	41
3	16 000	1.70	0.132	150	18

Since, as can be seen from Eq. (4), the amplitude of the torque A is proportional to $\partial S/\partial\theta$, Eq. (3) implies that the amplitude will be zero when $\vec{B}$ is in the $\langle 001\rangle$, $\langle 1\bar{1}1\rangle$, and $\langle 1\bar{1}0\rangle$ directions (i.e., $\theta = 0$, 54.8, and 90°, respectively). This was found to be true for our samples as can be seen from Figs. 1 and 2. Thus, our data provide a direct qualitative confirmation of the anisotropy of the conduction band.

A more detailed comparison between our data and the term which describes the warping of the conduction band[1] will be made next. In order to do so, it is useful to consider the amplitude of the torque oscillations to be expected from the results of theory[11] and experiment[8]

$$A \sim V\frac{\partial S}{\partial\theta}B^{1/2}e^{-\alpha_c/B}(T + T_i)\{\cos[g\hbar^2(dS/d\zeta)/4m_0]\}$$
$$\times\{\sinh[\pi c k_B(T + T_i)(dS/d\zeta)/\hbar eB]\}^{-1} , \quad (4)$$

where V is the volume of the sample, S is perpen-

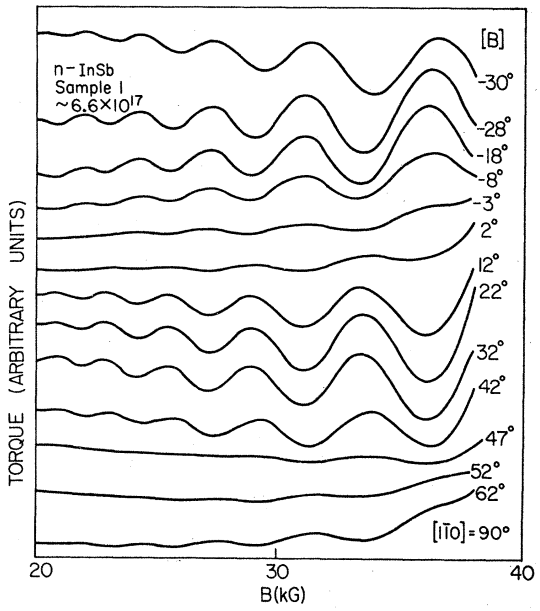

FIG. 1. Reproduction of recorder tracings of dHvA torque oscillations in n-InSb sample 1.

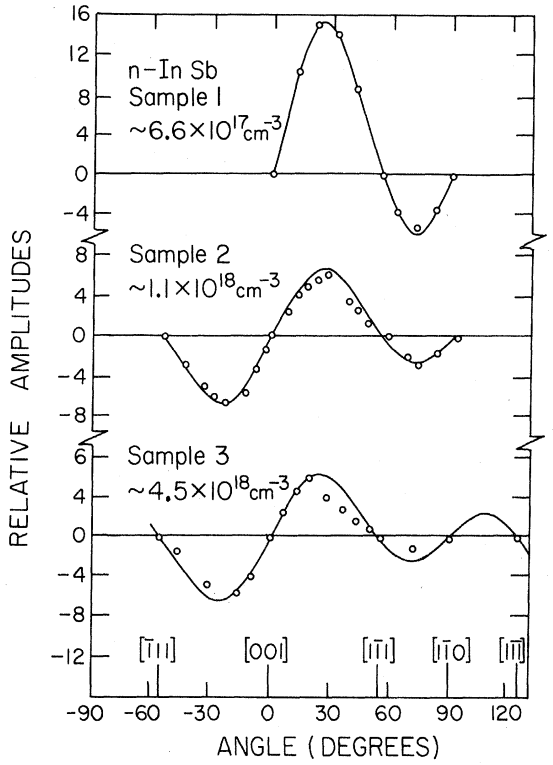

FIG. 2. Amplitude of dHvA torque oscillations vs orientation of the magnetic field for samples 1, 2, and 3 and curves showing the angular dependence of $\partial S/\partial\theta$ calculated from Eq. (3). Each calculated curve was made to fit a data point near maximum amplitude.

dicular to $\vec{B}$, α_c is the damping constant for collision broadening, T is the actual temperature, T_i is the apparent temperature associated with inhomogeneity broadening, g is the electronic g factor, m_0 is the electronic mass in free space, and $dS/d\zeta = (dS/dE)_E = \zeta$, where ζ is the Fermi energy. For n InSb, $dS/d\zeta$ and the g factor are expected to be almost independent of θ, and this expectation is borne out by the analysis of our data. Since our measurements indicate that, for a given direction of $\vec{B}$, $A \sim e^{-\alpha/B}$ with $\alpha \sim 2\alpha_c$ (see Tables II and IV), we infer that the argument of the hyperbolic sine must be large enough so that $1/\sinh t \approx 2\,e^{-t}$, where $t \equiv [\pi c k_B (T + T_i)(dS/d\zeta)/\hbar e B]$. We believe that the most appropriate way of analyzing our data employs this inference, and discussion of our results will be made accordingly. (Nevertheless, we have also deduced values for C_1 and $L - M - N$ for samples 1 and 2 assuming that $t \ll 1$. These are given in parentheses in Table IV.) From our measurements, α seems to be independent of θ so that the angular dependence of A must be due almost entirely to $\partial S/\partial\theta$. Figure 2 shows plots of relative amplitudes at a constant field value for three samples with different carrier concentrations. The circles represent the data points, and the curves were calculated from Eq. (3). Each curve was placed so as to fit the experimental data near a peak position. The excellent agreement of the calculated curves with the data indicates that warping is responsible for the anisotropy of the dHvA oscillations which we observe.

Further use of Eq. (4) will be made to deduce values of the anisotropy parameter C_1 of Eq. (1) for samples 1 and 2 by comparing the amplitudes observed for these samples with that of the highest-concentration sample (3).

We can deduce C_1 for sample 3 directly because

TABLE III. Measured and calculated periods of the dHvA torque oscillations for three n-InSb samples. P_{calc} is calculated from Eq. (5) using values of $1/|R_H e|$ from Table I.

Sample	Slice designation and shape of sample	P (10^{-6}G^{-1})	P_{calc} (10^{-6} G^{-1})
1	$W326$-J (brick)	4.6 ± 0.1	4.2
2	$W324$-H (cyl)	2.7 ± 0.2	3.0
3	$W226$-C (cyl)[a]	1.3 ± 0.1	1.2

[a]Brick-shaped sample from the same slice exhibited very similar characteristics.

TABLE IV. Information used and results obtained deducing the anisotropy of n-InSb samples 1 and 2 from the amplitude of dHvA torque oscillations using Eq. (7). Values for $x = g\hbar^2(dS/d\zeta)/4m_0$ are calculated from values in Table I. C_1 of sample 3 is deduced from the anisotropy of the period and is used in deducing C_1 for samples 1 and 2 (see text). $b^2 - 2c^2$ and y are calculated using equations in the Appendix and $L - M - N$ from C_1 using Eq. (8). The values of C_1 and $L - M - N$ in parentheses were calculated assuming $t \ll 1$ (see text).

Sample	$A_{\max}$ arb units	at	B (kG)	α (kG)	cos$x$	C_1	$b^2 - 2c^2$	y	$L - M - N$ / $\frac{\hbar^2}{2m_0}$
1	15.32		34.0	131	0.485	-0.104	-0.361	0.466	9.9
						(-0.062)			(5.9)
2	3.25		37.3	282	0.545	-0.46	-0.416	0.544	33
						(-0.32)			(22)
3	3.91		37.0	286	0.70	-0.25	-0.561	0.800	8.9

the dHvA period of this sample had a measurable dependence upon the direction of $\vec{B}$. In particular, the fractional change of period which occurred between $\theta = 5°$ and $\theta = 30°$ was 0.018 ± 0.001. Thus, since the period P is related to S by the relation[11]

$$P = 2\pi e/\hbar c S, \tag{5}$$

we obtain, by applying Eqs. (1) and (2), $C_1 = -0.25 \pm 0.015$ and $(S_{[1\bar{1}2]} - S_{[001]})/S_{[001]} = 0.023$. The anisotropy indicated by these values is different from that reported in Ref. 4 because in that work an error was made in deducing the fractional change of period and in the definition of the tabulated anisotropy. {The E quantity tabulated there was actually $[S(30°) - S(5°)]/S(5°)$}.

Equation (5) also provides a basis for calculating the average period of a sample from the Hall effect. Specifically, we have

$$P_{\text{calc}} = 2\pi e/\hbar c \bar{S} = 2e/\hbar c k_F^2 = 2e(|R_H e|/3\pi^2)^{2/3}/\hbar c, \tag{6}$$

where k_F is the average wave vector of an electron on the Fermi surface. Values of P_{calc} are given in Table III as mentioned before.

To deduce C_1 for samples 1 and 2 we first use Eqs. (3)–(5) to obtain

$$C_1 \sim A_{\max} P e^{\alpha/B}\{\sinh t\}/V \cos\left(g\hbar^2 \frac{dS}{d\zeta}\Big/4m_0\right) B^{1/2}(T + T_i). \tag{7}$$

The quantities $A_{\max}$, P, α, and V are obtained directly from measurements on our samples. All samples had approximately the same volume. Values of $A_{\max}$, P, and α are given in Tables III and IV and of $dS/d\zeta$ and g in Table I. The formula we used to calculate the $dS/d\zeta$ values was obtained by differentiating $S \approx \pi k_F^2$ with k_F^2 related to energy by Eq. (38) of Ref. 5. Values for g were calculated using a formula from the literature.[12] Values of the cosine factor are tabulated in Table IV.

Employing Eq. (7) and the tabulated information, we obtain for samples 1 and 2 the values of C_1 in Table IV. The significance of C_1 is that it can be used to deduce the band parameter $L - M - N$ from the relation

$$L - M - N \approx 16\, C_1/(b^2 - 2c^2)y, \tag{8}$$

where the factor of 16 and values for the parameters b, c, and y can be calculated from the Fermi energy and constants of the band structure by means of the equations in Ref. 5 and the Appendix. Identification of the various quantities involved and pertinent values of the band parameters are also given in Ref. 5 or the Appendix. For convenience, values of $b^2 - 2c^2$ and y are tabulated in Table IV.

The value of $L - M - N$ obtained from sample 3, $(8.9 \pm 0.7\ \hbar^2/2m_0)$, is the most significant since it depends on measurement of the period and the change of period with angle. It is almost within experimental error of the value of $(7.2 \pm 0.9)\ \hbar^2/2m_0$ obtained by Pidgeon and Groves[13] from magneto-optical measurements.

The values of $L - M - N$ obtained from samples 1 and 2 differ considerably from the value deduced from sample 3 (see Table IV). It is not clear why the discrepancies are quite so large, although they are undoubtedly due, at least partly, to the difficulty in obtaining from our data an accurate enough value of $e^{\alpha/B}$ for each sample.

B. Damping Factor

Now we shall discuss the size of α in the $e^{-\alpha/B}$ factor which describes the field dependence of our torque oscillations. Using results of theory for collision broadening[7] a calculated α_c can be obtained from

$$\alpha_c(\text{calc}) = \frac{\pi}{10^{-8}}\,\mu_0 \frac{\tau}{\tau_\rho}, \tag{9}$$

where μ_0 is the conductivity mobility in $\text{cm}^2/\text{V sec}$ and τ/τ_ρ is the ratio of the lifetime of an electron on the Fermi surface to the electrical resistivity relaxation time. The quantity μ_0 can be obtained from the Hall mobility $|R_H|/\rho_0$ measured at 4.2 K and τ/τ_ρ is given as a function of q_0/k_F in Ref. 7. Since the screening parameter q_0 is given[14] by $[4\pi e^2(dn/d\zeta)/K]^{1/2}$, where $dn/d\zeta$ is the density of energy states per unit volume at the Fermi energy and K is the static dielectric constant (≈ 16 for InSb), we obtain, using the nonparabolic density of states appropriate to InSb,[15]

$$q_0^2 = \frac{2e^2}{\pi K}\left(\frac{2m^*(0)}{\hbar^2}\right)^{3/2} \zeta^{1/2}\left(1 + \frac{\zeta}{E_g}\right)^{1/2} \times \left[1 + \left(2 - 5\frac{m^*(0)}{m_0}\right)\frac{\zeta}{E_g} - 8\frac{m^*(0)}{m_0}\left(\frac{\zeta}{E_g}\right)^2\right], \tag{10}$$

where $m^*(0)$ is the effective mass of electrons at the bottom of the conduction band ($\approx 013 m_0$ for InSb) and E_g is the width of the forbidden gap between the top of the valence band and the bottom of the conduction band (≈ 0.235 eV for InSb). For each sample, the q_0 calculated from Eq. (10) is used to obtain τ/τ_ρ from Eq. (47) of Ref. 7. Table II shows these quantities.

The α_c(calc) deduced from Eq. (9) are also given in Table II. It can be seen that they are much smaller than the respective experimental α given in Table IV.

One way to account for the differences is to suppose that the carrier concentration in the sample is not completely uniform. This effect has been characterized in terms of an inhomogeneity broadening[8] temperature T_i adding to the actual temper-

ature as indicated in Eq. (4) so that

$$\alpha - \alpha_c\,(\text{calc}) = \pi c k_B\,(T_i + T)\frac{dS}{d\xi}\Big/e\hbar\,. \qquad (11)$$

The T_i deduced using Eq. (11) are given in Table II. They are reasonable since the nonuniformity in concentration which they imply is much less than that detectable by measurements of the electrical potential or Hall effect as a function of position along each sample.

In order to obtain a more direct check on this inhomogeneity broadening interpretation, measurements at a much higher temperature would be needed. Unfortunately, we were able to make measurements only below the λ point of liquid He for the reasons indicated in Sec. II.

It is conceivable that some of the damping which we observe could be due to beats[16] arising because there are two sets of dHvA oscillations with slightly different periods due to the splitting of the conduction band caused by lack of inversion symmetry. However, such splitting occurs only in certain directions,[5,17] and it will be recalled that we did not find any measurable anisotropy in α.

It has been reported that Kondo scattering can influence the amplitude of dHvA oscillations in alloys.[18] Since n InSb exhibits some anomalies in its transport properties[19] which are similar to those connected with s-d scattering in metals, some analogous damping could possibly occur in n InSb. This idea must be regarded as highly speculative, however.

V. CONCLUSION

dHvA torque oscillations in n-InSb samples indicate that the conduction band is warped in the same manner as predicted by Kane's band model, yield a value of $8.9(\hbar^2/2m_0)$ for the $L-M-N$ band parameter, and imply the presence of both collision and inhomogeneity broadening of energy levels.

ACKNOWLEDGMENTS

The experimental part of this investigation was made possible by the hospitality of T. G. Berlincourt and the cooperation of A. S. Joseph of the Science Center, North American Rockwell Corporation.

APPENDIX

In this Appendix we give some additional formulas and information which are used in analyzing our data.

By straightforward use of Kane's three-band-approximation formula[5] for the energy of the conduction band, Seiler[20] has shown that

$$C_0 = (2m_0/\hbar^2)(E^2 + EE_g/w)/y$$

and

$$C_1 = y(b^2 - 2c^2)(L - M - N)/z\,,$$

where

$$w = 1 + k^2P_0^2\Delta/3(E_g+\Delta)^3\,,$$

$$y = 2E + [E_g - k^2P_0^2\Delta/3(E_g+\Delta)^2]/w\,,$$

$$z = (2m_0P_0^2/\hbar^2)\{[1 - \Delta(1+\gamma)/3(E_g+\Delta)] + E\Delta/3(E_g+\Delta)^2\} + yu\,,$$

$$\gamma = [E/(E_g+\Delta)]^3\{1/[1+E/(E_g+\Delta)]\}\,,$$

$$u = 1 + a^2A' + b^2M + c^2L'\,,$$

$$a = kP_0(E + E_g + \tfrac{2}{3}\Delta)/N_1\,,$$

$$b = (\sqrt{2}\Delta/3)E/N_1\,,$$

$$c = E(E + E_g + \tfrac{2}{3}\Delta)/N_1\,,$$

$$N_1 = [(E^2 + k^2P_0^2)(E + E_g + \tfrac{2}{3}\Delta)^2 + \tfrac{2}{9}E^2\Delta^2]^{1/2}\,.$$

Using the above expressions with $A' \approx -1$, $M = -5.6$, $L' = -2.6$, and $P_0 = 9.0\times10^{-8}$ eV cm, we obtained Eq. (8) of the text. The value of A' was chosen in view of the discussion in Appendix C of Ref. 1. Values for M, L', and P_0 were obtained from the paper cited in Ref. 13.

---

*Visiting Scientist at Science Center, North American Rockwell Corporation, Thousand Oaks, Calif.

†At Purdue partial support provided by the Advanced Research Projects Agency Interdisciplinary Laboratory Program.

[1]D. G. Seiler and W. M. Becker, Phys. Rev. 183, 784 (1969).

[2]G. A. Anticliffe and R. A. Stradling, Phys. Letters 20, 119 (1966).

[3]D. G. Seiler, Phys. Letters 31A, 309 (1970).

[4]A preliminary report was given by R. J. Sladek, A. S. Joseph, and E. Gertner, Phys. Letters 27A, 504 (1968).

[5]E. O. Kane, in *Semiconductors and Semimetals*, edited by R. K. Willardson and A. C. Beer (Academic, New York, 1966), Vol. 1, p. 75.

[6]R. B. Dingle, Proc. Roy. Soc. (London) A211, 517 (1952).

[7]A. D. Brailsford, Phys. Rev. 149, 456 (1966).

[8]B. L. Booth and A. W. Ewald, Phys. Rev. Letters 18, 491 (1967).

[9]A. S. Joseph and W. L. Gordon, Phys. Rev. 126, 489 (1962).

[10]A. S. Joseph and A. C. Thorsen, Phys. Rev. 133, A1546 (1964).

[11]I. M. Lifshitz and A. M. Kosevich, Zh. Eksperim.

i Teor. Fiz 29, 730 (1955) [Soviet. Phys. JETP 2, 636 (1956)].

[12]W. Zawadzki, Phys. Letters 4, 190 (1963).

[13]C. R. Pidgeon and S. H. Groves, Phys. Rev. 186, 824 (1969). These authors actually give $\gamma_3-\gamma_2$ which is $\frac{1}{6}(L-M-N)$.

[14]See, for example, J. E. Robinson and S. Rodriguez, Phys. Rev. 135, A779 (1964).

[15]H. Ehrenreich, J. Phys. Chem. Solids 2, 131 (1957).

[16]C. R. Whitsett, Phys. Rev. 138, A829 (1965); L. M. Roth, S. H. Groves, and P. W. Wyatt, Phys. Rev. Letters 19, 576 (1967); D. G. Seiler and W. M. Becker, Phys. Letters 26A, 96 (1967); and D. G. Seiler, W. M. Becker, and L. Roth, Phys. Rev. B 1, 764 (1970).

[17]R. L. Bell and K. T. Rogers, Phys. Rev. 152, 746 (1966).

[18]B. E. Paton and W. B. Muir, Phys. Rev. Letters 20, 732 (1968).

[19]See, for example, R. P. Khosla and R. J. Sladek, Phys. Rev. Letters 15, 521 (1965); and J. Phys. Soc. Japan Suppl. 21, 57 (1966).

[20]D. G. Seiler (unpublished).

PHYSICAL REVIEW B VOLUME 3, NUMBER 8 15 APRIL 1971

Zone-Boundary Acoustic Phonons in Adamantine Compounds from Far-Infrared Absorption Measurements

Glen A. Slack and S. Roberts

General Electric Research and Development Center, Schenectady, New York 12301

(Received 21 October 1970)

Optical-absorption studies in the far infrared at 4.2 °K have been made on single crystals of cubic ZnS, ZnSe, ZnTe, CdTe, and GaAs. Absorption peaks are seen which correspond to the creation of 2TA(L) and 2TA(X) phonons, allowed two-phonon processes in the zinc-blende structure. These same processes are forbidden in the diamond, rock-salt, and cesium-chloride structures. The TA(L), TA(X), LA(L), and LA(X) phonon energies for 12 different adamantine compounds can readily be correlated with the measured elastic constants by assuming that the phonon-dispersion curves for all the crystals are similar. From this correlation, some predictions are made for acoustic-phonon energies in GaSb, InP, and InAs. This correlation does not work well for either SiC or diamond crystals.

I. INTRODUCTION

Infrared studies of II-VI, III-V, IV-IV compounds and IVth column elements yield information about the phonon energies at critical points in the Brillouin zone. Studies of surface reflectivity or Raman scattering on bulk samples or absorption on thin films give values for the zone-center phonon energies TO(Γ) and LO(Γ). Since we will be concerned with only the cubic crystals, there are at most these two energies at the zone-center point Γ. Many optical-absorption studies at photon energies $\bar{\nu}$ above TO(Γ), i.e.,

$$\bar{\nu} > \mathrm{TO}(\Gamma), \tag{1}$$

show absorption peaks corresponding to the simultaneous generation of two or three or more phonons at various critical points. However, if we consider the photon region

$$\bar{\nu} < \mathrm{TO}(\Gamma), \tag{2}$$

some single- and multiple-phonon-generation peaks can also be present for the lower-energy phonons. Several authors have seen such absorption peaks, and have attributed them to one- and two-phonon-generation processes. Such data exist for ZnSe, CdTe, GaP, and InSb. These results as well as the results of Raman, neutron, and x-ray scattering are collected[1–42] in Table I. The labels TA and LA designate the transverse and longitudinal acoustic phonons at the various critical points[43] L, X, W, Σ. The identification of the zone-boundary critical points involved is made by a comparison of the optical results with those of neutron scattering for the crystals where both types of data are available. For the other crystals, the identification is less certain, and is based on analogies in the shape of the optical-absorption curves and in the values of the elastic constants of these adamantine compounds.

II. PRESENT RESULTS—FAR INFRARED

The optical-absorption curves of five different crystals in the far infrared are given in Fig. 1. All of the samples were single crystals. The CdTe was grown in this laboratory[44] from the melt.[45] The ZnTe and ZnSe were melt-grown crystals purchased from Eagle-Picher,[46] the ZnS was a natural cubic crystal,[47] and the GaAs was a melt-grown crystal from Monsanto.[48] The GaAs crystal was doped with about 10^{17} cm^{-3} of oxygen in order to give it a high electrical resistivity, and hence a very small free-